

## Accepted Manuscript

A novel and resumable Schiff-base fluorescent chemosensor for Zn(II)

Jun Yan, Long Fan, Jing-can Qin, Chao-rui Li, Zheng-yin Yang

PII: S0040-4039(16)30612-8

DOI: <http://dx.doi.org/10.1016/j.tetlet.2016.05.079>

Reference: TETL 47698

To appear in: *Tetrahedron Letters*

Received Date: 22 March 2016

Revised Date: 15 May 2016

Accepted Date: 20 May 2016



Please cite this article as: Yan, J., Fan, L., Qin, J-c., Li, C-r., Yang, Z-y., A novel and resumable Schiff-base fluorescent chemosensor for Zn(II), *Tetrahedron Letters* (2016), doi: <http://dx.doi.org/10.1016/j.tetlet.2016.05.079>

This is a PDF file of an unedited manuscript that has been accepted for publication. As a service to our customers we are providing this early version of the manuscript. The manuscript will undergo copyediting, typesetting, and review of the resulting proof before it is published in its final form. Please note that during the production process errors may be discovered which could affect the content, and all legal disclaimers that apply to the journal pertain.

# A novel and resumable Schiff-base fluorescent chemosensor for Zn(II)

Jun Yan, Long Fan, Jing-can Qin, Chao-rui Li, Zheng-yin Yang\*

College of Chemistry and Chemical Engineering, State Key Laboratory of Applied Organic Chemistry, Lanzhou University, Lanzhou 730000, P.R. China.

\*\*Corresponding author. Tel.: +86 931 8913515; Fax: +86 931 8912582; e-mail: [yangzy@lzu.edu.cn](mailto:yangzy@lzu.edu.cn) (Z.Y. Yang)

## Abstract:

A new resumable Schiff-base fluorescent probe 7-methoxychromone-3-carbaldehyde-(3'-hydroxy-2'-naphthaleneformyl) hydrazone (**L**) was designed and synthesized for selective recognition  $Zn^{2+}$ . With the titration and the ESI-MS spectra data, we reached the conclusion that the binding ratio between **L** and  $Zn^{2+}$  was determined to be 1. The sensor showed a strong fluorescence enhancement in ethanol system of  $Zn^{2+}$  (excitation 430 nm and emission 498 nm). And the enhancement may be due to C=N isomerization and Photoinduced Electron Transfer (PET).

**Keywords:** Fluorescent sensor; Reversibility; PET; C=N isomerization;  $Zn^{2+}$ .

## 1. Introduction

In recent years, with the increasingly deterioration of the environment, the toxic heavy metal ions are becoming more and more threatening to human health.<sup>1-5</sup> So it is of great significance to recognize heavy metal ions quickly and efficiently. Zinc ion, one of the eight most common heavy-metal pollution,<sup>6</sup> causes many severe diseases such as Parkinson's disease, Alzheimer's disease, and epilepsy if human ingest excessive amounts of it.<sup>7-10</sup> However, we cannot stop using Zinc in that it is also one of the most abundant transition-metal ions present in living cells and plays a very important role in variety of physiological and pathological processes such as regulation of metalloenzymes, gene expression, cell apoptosis and neural signal transmission.<sup>11-13</sup> Hence it is very important to develop highly selective and sensitive chemosensors for the detection of  $Zn^{2+}$  in production and our life.

Over the years there were many reported methods<sup>14-19</sup> to detect transition heavy metal ions, especially  $Zn^{2+}$  ions. Among these methods, fluorescent chemosensors have been paid much attention to detect metal ions because of their high response speed, good selectivity, high sensitive and easy operation character when mixed with these ions.<sup>20-25</sup> The design of fluorescent chemosensors for metal ions has attracted considerable attention in environmental researches and analytical fields. Schiff-base compounds and their metal complexes have been widely used in medicine, analytical chemistry, and the field of photochromic effect. What's more, as good ligands, Schiff-bases can be used to identify the content of metal ions and the quantitative analysis of metal ions.<sup>26-29</sup> In our study, 7-methoxychromone-3-carbaldehyde and 3-hydroxy-2-naphthoic acid hydrazide were selected as reactants to get the Schiff-base for both of them were widely used to synthesise chemosensors.<sup>30-32</sup> This Schiff-base was considered as a

potential fluorescent probe for the determination of metal cations.

Herein, we designed a new Schiff-base chemosensor **L** that allows the  $Zn^{2+}$  to be differentiated on the basis of distinct fluorescence responses in ethanol. The free **L** emitted very weak fluorescence due to the C=N isomerization and PET phenomena; while when bound with  $Zn^{2+}$ , the C=N isomerization and PET effects were inhibited and the molecular structure changed from flexible to rigid, which dramatically increased the fluorescence intensity.<sup>33-35</sup>

## 2. Experimental

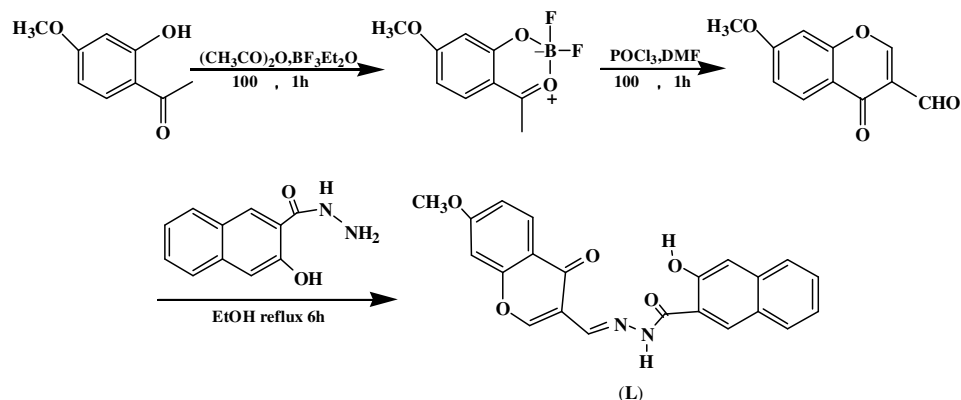
### 2.1. Materials and instrumentation

All chemicals were obtained from commercial suppliers and used without further purification. Fluorescence spectra were recorded on a Hitachi RF-4500 spectrophotometer equipped with quartz cuvettes of 1 cm path length. ESI-MS were determined on a Bruker esquire 6000 spectrometer. UV-Vis absorption spectra were determined on a Shimadzu UV-240 spectrophotometer.  $^1H$  NMR spectra were measured on the Bruker 400 MHz instruments using TMS as an internal standard.

### 2.2. Synthesis

7-methoxychromone-3-carbaldehyde was obtained according to the literature procedures.<sup>36</sup>

Synthesis of **L** was based on the following method (Scheme 1): an ethanol solution (12 mL) of



3-hydroxy-2-naphthoic acid hydrazide (0.101 g, 0.5 mmol) was added dropwise to a solution (25 mL) of 7-methoxychromone-3-carbaldehyde (0.102 g, 0.5 mmol) in ethanol. Then the solution was refluxed for 6 hrs under stirring and some white precipitant appeared. The mixture was filtered and dried under vacuum. Recrystallization from ethanol gave 7-methoxychromone-3-carbaldehyde-(3'-hydroxy-2'-naphthaleneformyl) hydrazone (**L**) which was dried under vacuum. Yield, 71.4%, m.p: 226–227°C.  $^1\text{H}$  NMR (DMSO- $d_6$ , 400 MHz):  $\delta$  12.03 (s, 1H, -NH-), 11.22 (s, 1H, -OH), 8.75 (s, 1H, H<sup>11</sup>), 8.55 (s, 1H, H<sup>2</sup>), 8.40 (s, 1H, H<sup>22</sup>), 8.00 (d,  $J = 8.0$  Hz, 1H, H<sup>5</sup>), 7.86 (d,  $J = 8.0$  Hz, 1H, H<sup>21</sup>), 7.72 (d,  $J = 8.0$  Hz, 1H, H<sup>18</sup>), 7.48 (t,  $J = 8.0$  Hz, 1H, H<sup>19</sup>), 7.33 (t,  $J = 8.0$  Hz, 1H, H<sup>20</sup>), 7.27 (s, 1H, H<sup>8</sup>), 7.19 (s, 1H, H<sup>17</sup>), 7.09 (d,  $J = 8.0$  Hz, 1H, H<sup>6</sup>), 3.87 (s, 3H, -CH<sub>3</sub>) (Figure S1). MS (ESI)  $m/z$  389.1 [M+H]<sup>+</sup>, (Figure S2).

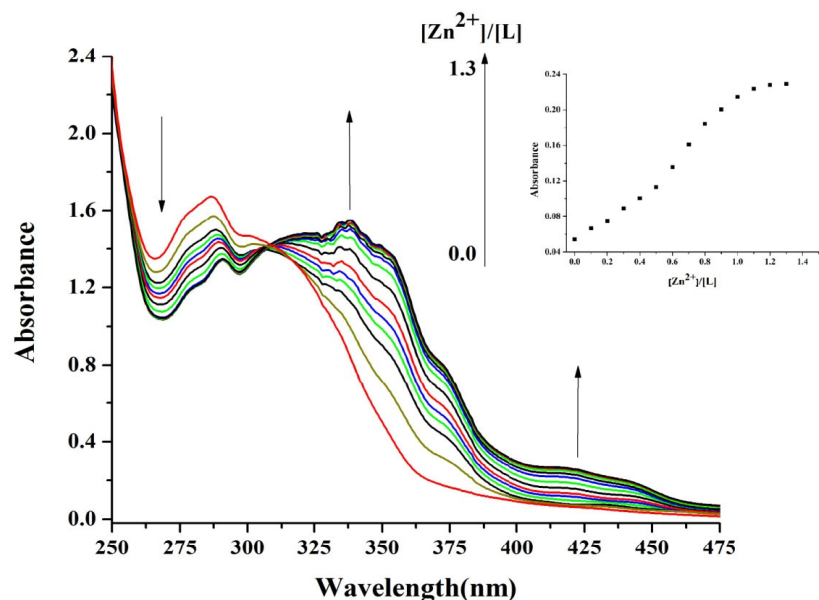
### 2.3. Analysis

Stock solutions (5.0 mM) of the nitrate salts of Al<sup>3+</sup>, Ba<sup>2+</sup>, Ca<sup>2+</sup>, Cu<sup>2+</sup>, Hg<sup>2+</sup>, Co<sup>2+</sup>, K<sup>+</sup>, Mg<sup>2+</sup>, Mn<sup>2+</sup>, Na<sup>+</sup>, Cr<sup>3+</sup>, Li<sup>+</sup>, Pb<sup>2+</sup>, Cd<sup>2+</sup>, Ag<sup>+</sup>, Fe<sup>3+</sup> and Zn<sup>2+</sup> in ethanol were prepared. Stock solutions of **L** (5.0 mM) were prepared in ethanol. Test solutions were prepared by placing 20  $\mu\text{L}$  of the probe stock solution into cuvettes, adding an appropriate aliquot of each ions stock, and diluting the solution to 2 mL with ethanol solutions. Both the excitation and emission slit widths were 3.0 nm.

## 3. Results and discussion

### 3.1. Absorption studies

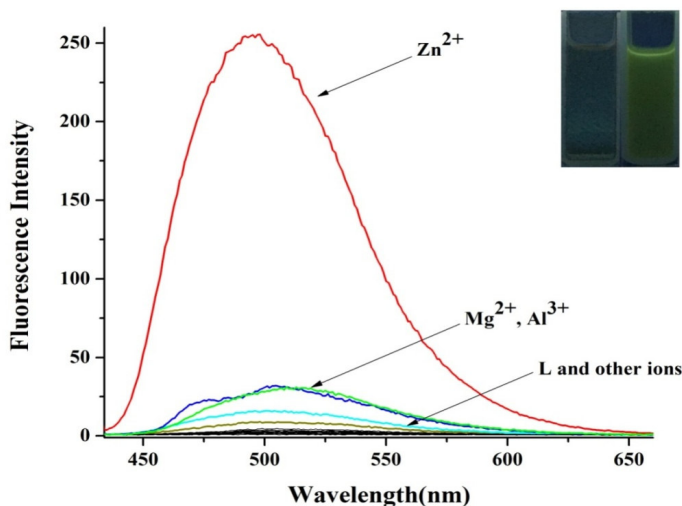
The binding properties of **L** with Zn<sup>2+</sup> were studied by UV-Vis titration in the above solution at room temperature (Figure 1). Upon addition of Zn<sup>2+</sup> ions (0-1.3 equiv.), the absorbance bands at 335 nm and 430 nm enhanced gradually while those at 268 nm lowered by



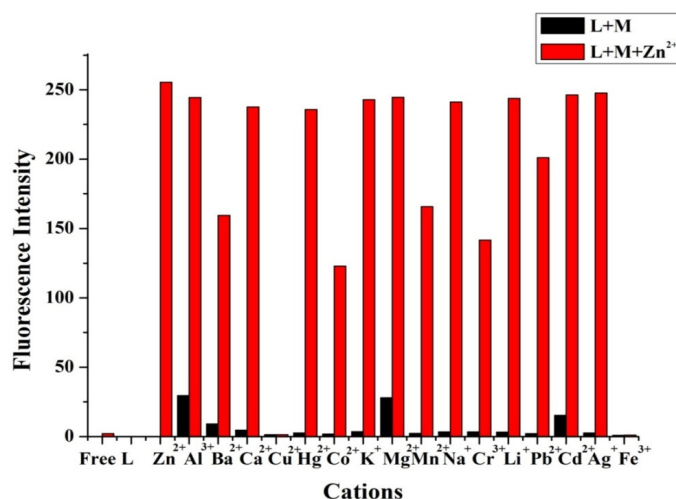
degrees. Moreover, there was clearly an isosbestic point at 307 nm, and the presence of the isosbestic point for the sensor suggested the formation of a complex.<sup>37-38</sup>

### 3.2. Emission studies

A fluorescence study was further used to determine the selectivity and sensitivity of **L** in the presence of various metal ions, such as  $\text{Al}^{3+}$ ,  $\text{Ba}^{2+}$ ,  $\text{Ca}^{2+}$ ,  $\text{Cu}^{2+}$ ,  $\text{Hg}^{2+}$ ,  $\text{Co}^{2+}$ ,  $\text{K}^+$ ,  $\text{Mg}^{2+}$ ,  $\text{Mn}^{2+}$ ,  $\text{Na}^+$ ,  $\text{Cr}^{3+}$ ,  $\text{Li}^+$ ,  $\text{Pb}^{2+}$ ,  $\text{Cd}^{2+}$ ,  $\text{Ag}^+$ ,  $\text{Fe}^{3+}$  and  $\text{Zn}^{2+}$ . Fascinatingly, the treatment of **L** (50.0  $\mu\text{M}$ ) with  $\text{Zn}^{2+}$  (50.0  $\mu\text{M}$ ) resulted in a strong increase in the fluorescence intensity in the emission spectrum at 498 nm upon excitation at 430 nm (Figure 2). And interestingly, no such effect was observed when **L** was treated with other cations (50.0  $\mu\text{M}$ ). The probe exhibited high selectivity for  $\text{Zn}^{2+}$  over other metal ions.



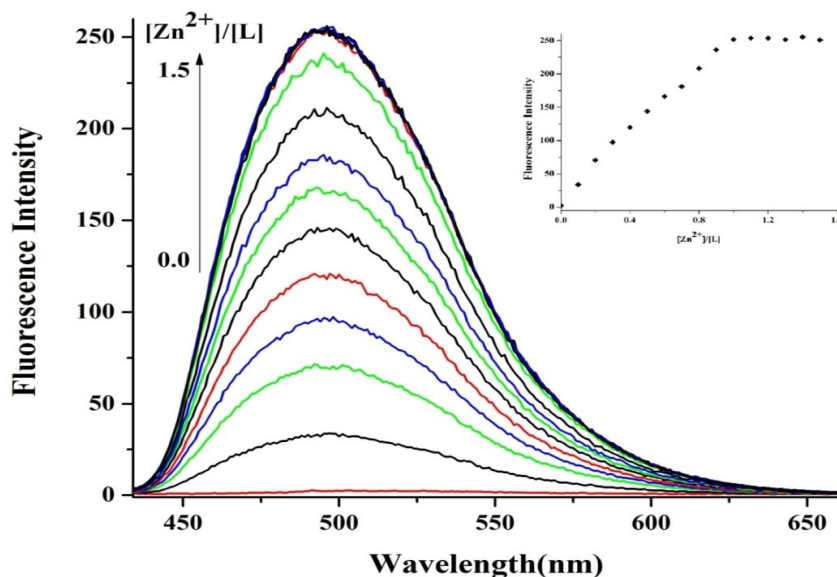
To explore the possibility of using **L** as a practical ion selective fluorescent chemosensor for  $\text{Zn}^{2+}$ , competition experiments were carried out. For this purpose, **L** was treated with  $\text{Zn}^{2+}$  (50.0  $\mu\text{M}$ ) in the presence of other metal ions (50.0  $\mu\text{M}$ ), such as  $\text{Al}^{3+}$ ,  $\text{Ba}^{2+}$ ,  $\text{Ca}^{2+}$ ,  $\text{Cu}^{2+}$ ,  $\text{Hg}^{2+}$ ,  $\text{Co}^{2+}$ ,  $\text{K}^+$ ,  $\text{Mg}^{2+}$ ,  $\text{Mn}^{2+}$ ,  $\text{Na}^+$ ,  $\text{Cr}^{3+}$ ,  $\text{Li}^+$ ,  $\text{Pb}^{2+}$ ,  $\text{Cd}^{2+}$ ,  $\text{Ag}^+$  and  $\text{Fe}^{3+}$ . As shown in Figure 3, good



selectivity of **L** was displayed in the presence of most metal ions, except for two metal ions  $\text{Fe}^{3+}$  and  $\text{Cu}^{2+}$  that are well known as the strong quenchers of fluorescence. The fluorescence of the **L-Zn<sup>2+</sup>** system was quenched, which might be due to an energy or electron transfer.<sup>39</sup> As reported in the literature,<sup>40-41</sup> it was possibly because the newly formed complex **L-Fe<sup>3+</sup>** or

**L**-Cu<sup>2+</sup> was too stable to be replaced by Zn<sup>2+</sup>.

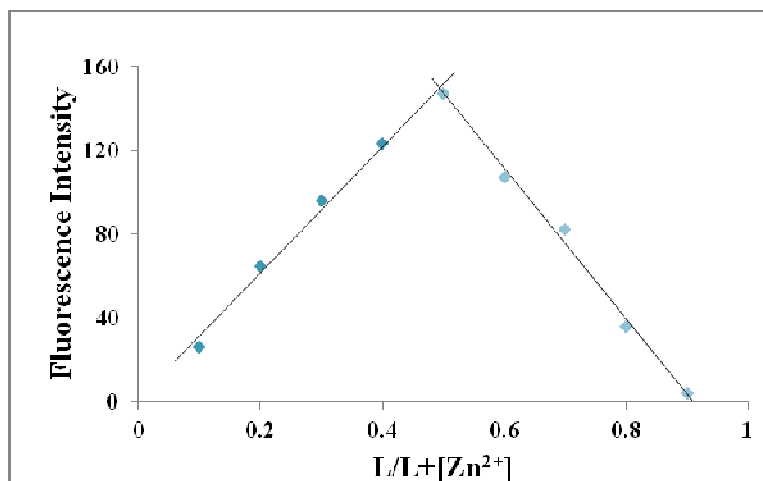
In Figure 4, the free **L** (50.0 μM, λ<sub>ex</sub> = 430 nm) emitted very weak fluorescence due to the



C=N isomerization and PET phenomena. Upon addition of Zn<sup>2+</sup>, a strong fluorescence enhancement was observed at 498 nm. And the stoichiometry of **L**-Zn<sup>2+</sup> complex was determined by changes in the fluorogenic response in the presence of varying Zn<sup>2+</sup> concentrations. After the addition of 1.0 equiv. of Zn<sup>2+</sup>, the fluorescence spectrum reached a saturation level. The saturation behavior of **L** with Zn<sup>2+</sup> indicated that the **L**-Zn<sup>2+</sup> complex has a 1:1 stoichiometry.

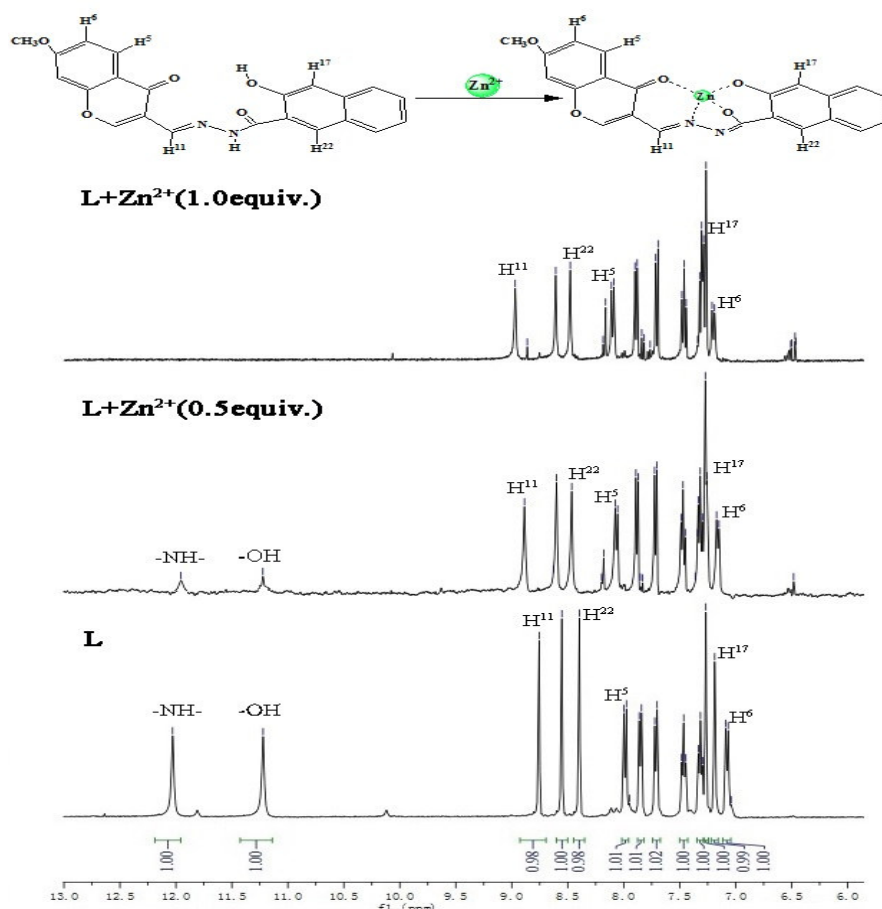
### 3.3. Binding studies

In order to obtain more evidence to determine the stoichiometry between **L** and Zn<sup>2+</sup>, the method of continuous variation (Job's plot) was used.<sup>42</sup> The total concentration of the **L** and Zn<sup>2+</sup> was constant (50.0 μM), with a continuous variable molar fraction of guest ( $[L] / [L] + [Zn^{2+}]$ ). Figure 5 shows the Job's plot of **L** with Zn<sup>2+</sup> (at 498 nm) and reveals that the **L**-Zn<sup>2+</sup> complex

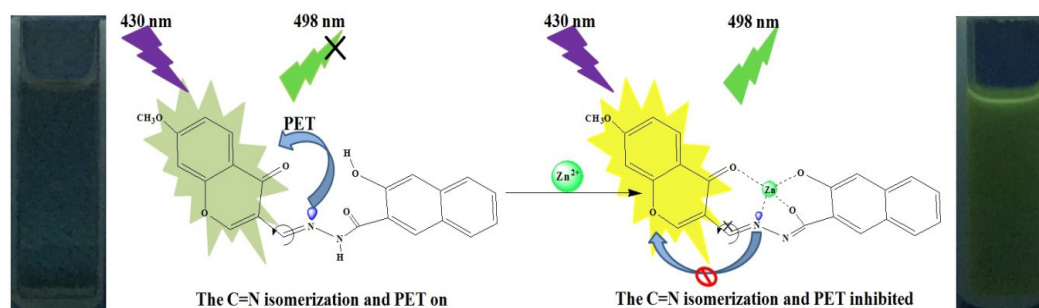


concentration approaches a maximum when the molar fraction of  $\text{Zn}^{2+}$  is 0.5, which means **L** and  $\text{Zn}^{2+}$  forms a 1:1 complex. In addition, the formation of a 1:1 complex between **L** and  $\text{Zn}^{2+}$  was further conformed by the appearance of a peak at  $m/z$  452.5 that is assignable to  $[\text{L} + \text{Zn}^{2+} - \text{H}^+]^+$  in the ESI-MS spectra (Figure S3).

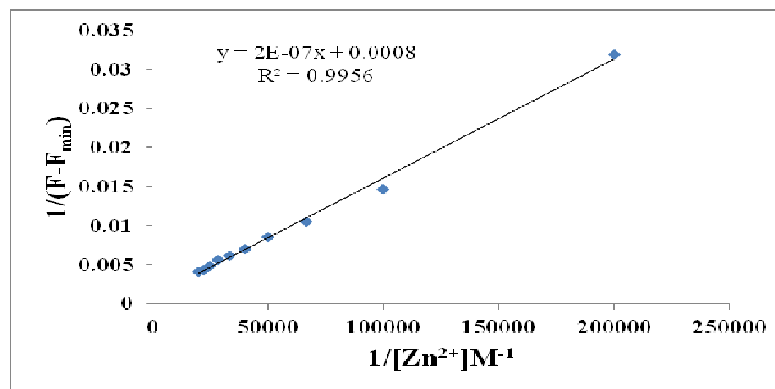
NMR studies provided additional evidence of the interaction between **L** and  $\text{Zn}^{2+}$ .  $^1\text{H}$  NMR spectra of **L** were recorded in  $\text{DMSO-d}_6$  upon the addition of  $\text{Zn}^{2+}$ . Significant spectral changes were observed as shown in Figure 6. Peaks for the protons of -NH- and -OH gradually disappeared, which indicated the enolization and deprotonation of the ligand in the presence of  $\text{Zn}^{2+}$ .<sup>43-44</sup> The signals of  $\text{H}^5$ ,  $\text{H}^{11}$ ,  $\text{H}^{17}$  and  $\text{H}^{22}$  were downfield shifted 0.11, 0.22, 0.07, 0.08 respectively, while signals of the other protons remained nearly unchanged. These phenomena indicated that the hydroxyl group, carbonyl group and CN group coordinated with  $\text{Zn}^{2+}$ , which changed the electron distribution in the chemosensor. Furthermore, there were a number of small signals for the aryl protons coming into being, such as the signal peaks of  $\delta$  8.86,  $\delta$  8.16,  $\delta$  7.84,  $\delta$  6.50 and so on, which showed a slight change for the system upon the addition of  $\text{Zn}^{2+}$ . The  $^1\text{H}$  NMR data gave the conclusion that the binding of **L** to  $\text{Zn}^{2+}$  generated a rigid structure through a



chelating reaction so that the C=N isomerization and PET effects were inhibited (Figure 7).



As shown in Figure 8, the association constant  $K_a$  of the complex was then calculated to be



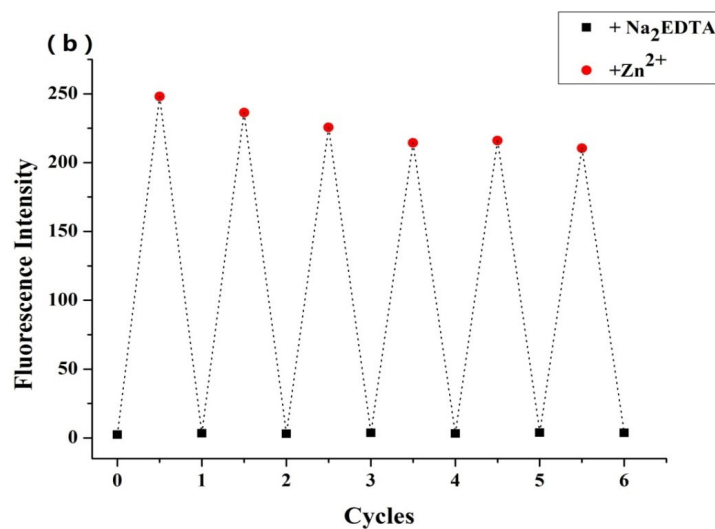
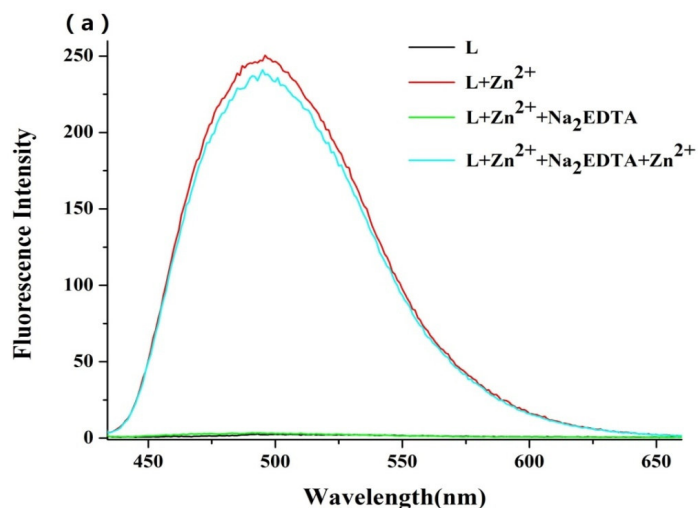
$2.0 \times 10^4 \text{ M}^{-1}$  with a linear relationship by Benesi-Hildebrand equation (Eq. (1)).<sup>45</sup>

$$\frac{1}{F - F_{\min}} = \frac{1}{K(F_{\max} - F_{\min})[\text{Zn}^{2+}]} + \frac{1}{F_{\max} - F_{\min}} \quad (1)$$

where  $F_{\max}$ ,  $F$  and  $F_{\min}$  are fluorescence intensities of **L** in the presence of  $\text{Zn}^{2+}$  at saturation, any intermediate  $\text{Zn}^{2+}$  concentration, and free **L**.

The detection limit of **L** for the analysis of  $\text{Zn}^{2+}$  was also calculated based on the fluorescence titration. As shown in Figure S4, according to the following equation: detection limit =  $3\sigma/k$ ,<sup>46</sup> the detection limit reached at  $1.73 \times 10^{-7} \text{ M}$ . Where  $\sigma$  was the standard deviation of blank measurements, and  $k$  was the slope between fluorescence intensity versus sample concentration.

Reversibility is a prerequisite in developing novel chemosensors for practical application. The reversibility of the recognition process of **L** was performed by adding  $\text{Zn}^{2+}$  bonding agent and  $\text{Na}_2\text{EDTA}$ . The addition of  $\text{Na}_2\text{EDTA}$  to a mixture of **L** and  $\text{Zn}^{2+}$  resulted in diminution of the fluorescence intensity, which indicated the regeneration of the free chemosensor **L**. Upon addition of  $\text{Zn}^{2+}$  again, the fluorescence was recovered. After several cycles, the chemosensor still showed excellent restorability with little fluorescent efficiency loss (Figure 9). Such reversibility and regeneration are important for the fabrication of devices to sense the  $\text{Zn}^{2+}$  ions.



#### 4. Conclusion

In summary, we have developed a novel chemosensor **L** based on the C=N isomerization and PET mechanism. The probe exhibited high selectivity for Zn<sup>2+</sup> over other metal ions with a strong fluorescence enhancement and high sensitivity with the detection limit reaching at 10<sup>-7</sup> M level in ethanol. This discovery of the dramatically enhanced fluorescence is probably due to the formation of a 1:1 complex **L-Zn<sup>2+</sup>** in which the C=N isomerization and PET effects are inhibited. Moreover, the chemosensor still showed excellent restorability. Thus, we believe **L** has the ability to serve as a potential sensor for Zn<sup>2+</sup> detection. This strategy may provide a

general way for designing new sensors to detect other environmentally and biologically relevant species.

ACCEPTED MANUSCRIPT

### **Acknowledgments**

This work is supported by the National Natural Science Foundation of China (81171337) and Gansu NSF (1308RJZA115).

**References**

1. Sakamoto, M.; Nakano, A.; Akagi, H. *Environ. Res.* **2001**, *87*, 92-98.
2. Waalkes, M. P. *J. Inorg. Biochem.* **2000**, *79*, 241-244.
3. Chen, H.; Teng, Y.; Lu, S.; Wang, Y.; Wang, J. *Sci. Total Environ.* **2015**, *512-513*, 143-153.
4. Omar, N. A.; Praveena, S. M.; Aris, A. Z.; Hashim, Z. *Food Chem.* **2015**, *188*, 46-50.
5. Koupaie, E. H.; Eskicioglu, C. *J. Hazard. Mater.* **2015**, *300*, 855-865.
6. Ang, H. H. *Food Chem. Toxicol.* **2008**, *46*, 1969-1975.
7. Smith, J. L.; Xiong, S.; Markesbery, W. R.; Lovell, M. A. *Neuroscience* **2006**, *140*, 879-888.
8. Jiang, P.; Guo, Z. *Coord. Chem. Rev.* **2004**, *248*, 205-229.
9. Ho, E. *J. Nutr. Biochem.* **2004**, *15*, 572-578.
10. Bush, A. I.; Pettingell, W. H.; Paradis, M. D.; Tanzi, R. E. *J. Biol. Chem.* **1994**, *269*, 12152-12158.
11. Hu, Q.; Tan, Y.; Liu, M.; Yu, J.; Cui, Y.; Yang, Y. *Dyes Pigments* **2014**, *107*, 45-50.
12. Yan, M. H.; Li, T. R.; Yang, Z. Y. *Inorg. Chem. Commun.* **2011**, *14*, 463-465.
13. Sladek, R. *Nature* **2007**, *445*, 881-885.
14. Ghaedi, M.; Ahmadi, F.; Shokrollahi, A. *J. Hazard. Mater.* **2007**, *142*, 272-278.
15. Zeeb, M.; Sadeghi, M. *Microchim. Acta* **2011**, *175*, 159-165.
16. Bottcher, A.; Takeuchi, T.; Hardcastle, K. I.; Meade, T. J.; Gray, H. B. *Inorg. Chem.* **1997**, *36*, 2498-2504.
17. Panayi, A. E.; Spyrou, N. M.; Iversen, B. S.; White, M. A.; Part, P. *J. Neurosci.* **2002**, *195*, 71-76.
18. Boevski, I. V.; Daskalova, N.; Havezov, I. *Spectrochim. Acta, Part B* **2000**, *55*, 1643-1657.

19. Gulaboski, R.; Mirceski, V.; Scholz, F. *Electrochem. Commun.* **2002**, *4*, 277-283.
20. Ma, Y.; Liu, H.; Liu, S.; Yang, R. *Analyst* **2012**, *137*, 2313-2317.
21. Valeur, B.; Leray, I. *Coord. Chem. Rev.* **2000**, *205*, 3-40.
22. Samanta, S.; Goswami, S.; Ramesh, A.; Das, G. *Sens. Actuators, B* **2014**, *194*, 120-126.
23. Mei, L.; Xiang, Y.; Li, N.; Tong, A. J. *Talanta* **2007**, *72*, 1717-1722.
24. Liu, C. J.; Yang, Z. Y.; Yan, M. H. *J. Coord. Chem.* **2012**, *65*, 3845-3850.
25. Park, G. J.; Lee, J. J.; You, G. R.; Nguyen, L. T.; Noh, I.; Kim, C. *Sens. Actuators, B* **2016**, *223*, 509-519.
26. Wen, H.; Niu, H.; Li, B.; Ma, X.; Bai, X.; Zhang, Y.; Wang, W. *Synth. Met.* **2015**, *202*, 89-97.
27. Vikneswaran, R.; Syafiq, M. S.; Eltayeb, N. E.; Kamaruddin, M. N.; Ramesh, S.; Yahya, R. *Spectrochim. Acta, Part A* **2015**, *150*, 175-180.
28. Zhang, Y. G.; Shi, Z. H.; Yang, L. Z.; Tang, X. L.; An, Y. Q.; Ju, Z. H.; Liu, W. S. *Inorg. Chem. Commun.* **2014**, *39*, 86-89.
29. Song, Z. K.; Dong, B.; Lei, G. J.; Peng, M. J.; Guo, Y. *Tetrahedron Lett.* **2013**, *54*, 4945-4949.
30. Fan, L.; Qin, J.; Li, T.; Wang, B.; Yang, Z. *Sens. Actuators, B* **2014**, *203*, 550-556.
31. Park, G. J.; Na, Y. J.; Jo, H. Y.; Lee, S. A.; Kim, A. R.; Noh, I.; Kim, C. *New J. Chem.* **2014**, *38*, 2587-2594.
32. Zhao, Y.; Lin, Z.; Ou, S.; Duan, C.; Liao, H.; Bai, Z. *Inorg. Chem. Commun.* **2006**, *9*, 802-805.
33. Tang, K. C.; Chang, M. J.; Lin, T. Y.; Pan, H. A.; Fang, T. C.; Chen, K. Y.; Hung, W. Y.;

- Hus, Y. H.; Chou, P. T. *J. Am. Chem. Soc.* **2011**, *133*, 17738-17745.
34. Wu, J. S.; Liu, W. M.; Zhuang, X. Q.; Wang, F.; Wang, P. F.; Tao, S. L.; Zhang, X. H.; Wu, S. K.; Lee, S. T. *Org. Lett.* **2007**, *9*, 33-36.
35. Fujikawa, Y.; Urano, Y.; Komatsu, T.; Hanaoka, K.; Kojima, H.; Terai, T.; Inoue, H.; Nagano, T. *J. Am. Chem. Soc.* **2008**, *130*, 14533-14543.
36. Hogberg, T.; Vora, M.; Drake, S. D.; Mitscher, L. A.; Chu, D. T. W. *Acta Chem. Scand., B* **1984**, *38*, 359-366.
37. Marnett, M.; Aragoni, M. C.; Lippolis, V. *Inorg. Chem.* **2009**, *48*, 9236-9249.
38. Guha, S.; Lohar, S.; Sahana, A.; Banerjee, A.; Safin, D. A.; Babashkina, M. G.; Mitoraj, M. P.; Bolte, M.; Garcia, Y.; Mukhopadhyay, S. K.; Das, D. *Dalton Trans.* **2013**, *42*, 10198-10207.
39. Martinez, R.; Molina, P. *Org. Lett.* **2005**, *7*, 5869-5872.
40. Burdette, S. C.; Frederickson, C. J.; Bu, W.; Lippard, S. J. *J. Am. Chem. Soc.* **2003**, *125*, 1778-1787.
41. Liu, W.; Xu, L.; Sheng, R.; Wang, P.; Li, H.; Wu, S. *Org. Lett.* **2007**, *9*, 3829-3832.
42. Kim, S. H.; Choi, H. S.; Kim, J.; Lee, S. J.; Quang, D. T.; Kim, J. S. *Org. Lett.* **2010**, *12*, 560-563.
43. Monfared, H. H.; Falakian, H.; Bikas, R.; Mayer, P. *Inorg. Chim. Acta* **2013**, *394*, 526-534.
44. Xiao, W.; Lu, Z. L.; Wang, X. J.; Su, C. Y.; Yu, K. B.; Liu, H. Q.; Kang, B. S. *Polyhedron* **2000**, *19*, 1295-1304.
45. Benesi, H. A.; Hildebrand, J. H. *J. Am. Chem. Soc.* **1949**, *71*, 2703-2707.
46. Samanta, S.; Goswami, S.; Ramesh, A.; Das, G. *Sens. Actuators, B* **2014**, *194*, 120-126.

**Figure captions**

**Figure 1.** UV-Vis absorption spectra of **L** in EtOH (50.0  $\mu\text{M}$ ) upon the addition of  $\text{Zn}(\text{NO}_3)_2$  (0-1.2 equiv.). Inset: Absorption intensity of **L** at 430 nm as a function of (0-1.3 equiv.)  $\text{Zn}^{2+}$  concentration.

**Figure 2.** Fluorescence responses of **L** (50.0  $\mu\text{M}$ ) in EtOH with 50.0  $\mu\text{M}$  of  $\text{Al}^{3+}$ ,  $\text{Ba}^{2+}$ ,  $\text{Ca}^{2+}$ ,  $\text{Cu}^{2+}$ ,  $\text{Hg}^{2+}$ ,  $\text{Co}^{2+}$ ,  $\text{K}^+$ ,  $\text{Mg}^{2+}$ ,  $\text{Mn}^{2+}$ ,  $\text{Na}^+$ ,  $\text{Cr}^{3+}$ ,  $\text{Li}^+$ ,  $\text{Pb}^{2+}$ ,  $\text{Cd}^{2+}$ ,  $\text{Ag}^+$ ,  $\text{Fe}^{3+}$  and  $\text{Zn}^{2+}$  ( $\lambda_{\text{ex}}=430$  nm). Inset: fluorescence emission color and intensity changes of the sensor (50.0  $\mu\text{M}$ ) in the absence and presence of  $\text{Zn}^{2+}$  (50.0  $\mu\text{M}$ ).

**Figure 3.** Relative fluorescence of **L** and its complexation with  $\text{Zn}^{2+}$  in the presence of various metal ions in EtOH. Black bar: **L** (50.0  $\mu\text{M}$ ) and **L** with 1.0 equiv. of  $\text{Al}^{3+}$ ,  $\text{Ba}^{2+}$ ,  $\text{Ca}^{2+}$ ,  $\text{Cu}^{2+}$ ,  $\text{Hg}^{2+}$ ,  $\text{Co}^{2+}$ ,  $\text{K}^+$ ,  $\text{Mg}^{2+}$ ,  $\text{Mn}^{2+}$ ,  $\text{Na}^+$ ,  $\text{Cr}^{3+}$ ,  $\text{Li}^+$ ,  $\text{Pb}^{2+}$ ,  $\text{Cd}^{2+}$ ,  $\text{Ag}^+$ ,  $\text{Fe}^{3+}$  stated. Red bar: 50.0  $\mu\text{M}$  of **L** and 1.0 equiv. of  $\text{Zn}^{2+}$  in the presence of 1.0 equiv. of other metal ions stated ( $\lambda_{\text{ex}}=430$  nm).

**Figure 4.** Fluorescence spectra of **L** (50.0  $\mu\text{M}$ ) with addition of increasing amount of  $\text{Zn}^{2+}$  (0-1.5 equiv.) in EtOH ( $\lambda_{\text{ex}}=430$  nm, slit: 3 nm / 3 nm). Inset: Fluorescence emission intensity of **L** at 498 nm as a function of (0-1.5 equiv.)  $\text{Zn}^{2+}$  concentration.

**Figure 5.** Job's plot of **L** in EtOH showing 1:1 stoichiometry of the complex between **L** and  $\text{Zn}^{2+}$ . The total concentration of **L** and  $\text{Zn}^{2+}$  is 50.0  $\mu\text{M}$ . Fluorescence emission intensity is recorded at 498 nm.

**Figure 6.**  $^1\text{H}$  NMR spectra of **L** with  $\text{Zn}(\text{NO}_3)_2 \cdot 6\text{H}_2\text{O}$  in  $\text{DMSO-d}_6$ : (I) **L** (bottom); (II) **L** with  $\text{Zn}^{2+}$  (top).

**Figure 7.** Proposed binding mode for interaction of  $\text{Zn}^{2+}$  with **L**.

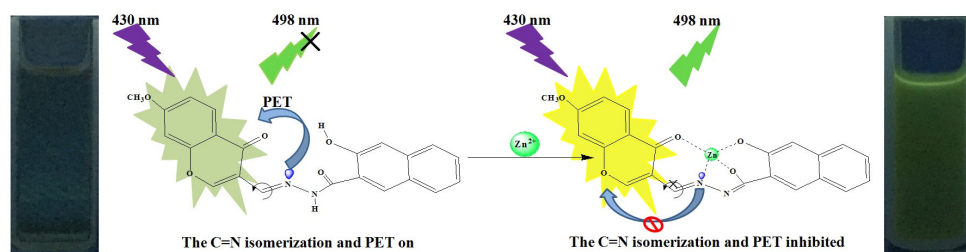
**Figure 8.** Benesi-Hildebrand analysis of the emission changes for the complexation between **L**

and  $\text{Zn}^{2+}$ .

**Figure 9.** (a) Fluorescence spectra of **L** (50.0  $\mu\text{M}$ ) upon the sequential addition of  $\text{Zn}^{2+}$  and  $\text{Na}_2\text{EDTA}$  (1.0 equiv.) in ethanol. (b) Reversible changes in fluorescence intensity of **L** (50.0  $\mu\text{M}$ ) at 498 nm after the sequential addition of  $\text{Zn}^{2+}$  and  $\text{Na}_2\text{EDTA}$  (1.0 equiv.).

**Scheme 1.** Synthesis of 7-methoxychromone-3-carbaldehyde-(3'-hydroxy-2'-naphthaleneformyl) hydrazone (**L**).

ACCEPTED MANUSCRIPT



Proposed binding mode for interaction of  $Zn^{2+}$  with **L**.

ACCEPTED MANUSCRIPT

- An easy-to-make Schiff-base fluorescent sensor was designed and synthesized.
- The probe exhibited high selectivity and sensitivity for  $\text{Zn}^{2+}$  over other metal ions.
- The chemosensor showed excellent restorability.
- C=N isomerization and PET can be used to explain the high selectivity of the probe.

ACCEPTED MANUSCRIPT